Delaney *et al. Herit Sci (2018) 6:31*
https://doi.org/10.1186/s40494-018-0197-y

Heritage Science

RESEARCH ARTICLE

Open Access

Integrated X-ray fluorescence and diffuse visible-to-near-infrared reflectance scanner for standoff elemental and molecular spectroscopic imaging of paints and works on paper

John K. Delaney[1*], Damon M. Conover[1,2,3], Kathryn A. Dooley[1], Lisha Glinsman[1], Koen Janssens[4] and Murray Loew[2]

Abstract

Prior studies have shown the improved ability to identify artists' pigments by combining results from X-ray fluorescence (XRF), which provides elemental information, with reflectance spectroscopy in the visible to near infrared (400–1000 nm) that provides information on electronic transitions. Extending the spectral range of reflectance spectroscopy into the UV, 350–400 nm, allows identification of several white pigments since their electronic transitions occur in this region (e.g., zinc white and rutile and anatase forms of titanium white). Extending the range further into the infrared, out to 2500 nm, provides information on vibrational transitions of various functional groups, such as hydroxyl, carbonate, and methyl groups. This allows better identification of mineral-based pigments and some paint binders. The combination of elemental information with electronic and vibrational transitions provides a more robust method to identify artists' materials in situ. The collection of both sets of spectral information across works of art, such as paintings and works on paper, allows generating a more complete map of artists' materials. Here, we describe a 2-D scanner that simultaneously collects XRF spectra and reflectance spectra from 350 to 2500 nm across the surfaces of works of art. The scanner consists of a stationary, single pixel XRF spectrometer and fiber optic reflectance spectrometer along with a 2-D position-controlled easel that moves the artwork in front of the two detection systems. The dual-mode scanner has been tested on a variety of works of art from illuminated manuscripts (0.1×0.1 m^2) to paintings as large as 1.7×1.9 m^2. The scanner is described and two sets of results are presented. The first is the XRF scanning of a large warped panel painting by Andrea del Sarto titled *Charity*. The second is a combined XRF and reflectance scan of Georges Seurat's painting titled *Haymakers at Montfermeil*. The XRF was collected at 1 mm spatial sampling and the reflectance spectral data at 3 mm. Combining the results from the data sets was found to enhance the identification of pigments as well as yield distribution maps, in spite of the relatively low reflectance spatial sampling. The elemental and reflectance maps allowed the identification and mapping of lead white, cobalt blue, viridian, ochres, and likely chrome yellow. The maps also provide information on the mixing of pigments. While the reflectance image cube has 10–20× larger spatial samples than desired, the elimination of having to use two hyperspectral cameras to cover the range from 400 to 2500 nm makes for a low cost dual modality scanner.

Keywords: Reflectance imaging spectroscopy, MA-XRF, X-ray fluorescence, FORS, Pigment mapping

*Correspondence: j-delaney@nga.gov
[1] Department of Scientific Research, National Gallery of Art, Washington, DC 20565, USA
Full list of author information is available at the end of the article

Background

Fiber-optic reflectance spectroscopy (FORS) and X-ray fluorescence (XRF) spectroscopy are non-invasive point-based analytical methods that can be utilized in artists' material identification. Both FORS and XRF spectroscopy are common and valuable tools in the analysis of artists' materials. FORS provides information regarding the electronic and vibrational transitions of molecules, while XRF spectroscopy can be used to identify elemental composition [1]. Both, however, have the same limitations of other point-based analytical methods: (1) using materials identified at one point to infer the presence of materials at another point can lead to errors, and (2) point measurements do not show the spatial distribution of materials. These limitations can be addressed by constructing a scanner, in which each modality is moved in front of a painting, and spectra are collected at regularly-spaced intervals. XRF imaging spectroscopy point scanners, also known in the cultural heritage field as Macro-XRF instruments, have been developed and used to produce two-dimensional elemental maps of paintings, stained glass windows and works on paper [2–4]. Separately hyperspectral cameras have been configured to provide reflectance image cubes of works of art to assist in pigment identification and mapping [5].

At the National Gallery of Art, Washington, D.C., an XRF imaging spectroscopy scanner was constructed in 2014 based on the design of the University of Antwerp's scanner [2–4] but with one important modification. Rather than moving the X-ray source and detector, the National Gallery of Art (Gallery) scanner utilizes a computer-controlled, position control loop, two-axis easel to move the artwork, while the X-ray source and detector remain stationary. This allows large areas to be scanned (1.7×1.4 m^2). This scanner has been used to collect XRF spectra and make elemental maps of several paintings [5–9], although this work was done with a lower power X-ray source having a 65-micrometer spot size that has been replaced as described here. Since the original development of the Gallery's XRF scanner, a variety of non-commercial, XRF scanners for cultural heritage science have been developed based on laboratory X-ray sources. Ravaud et al. [10] have developed a highly portable XRF scanner without sacrificing performance. More advanced scanners, such as one developed by Romano et al. [11], which provide high scan rates with confocal X-ray optics, and on-the-fly fitting of the XRF spectra have been constructed.

One of the motivations in building a position-controlled easel that moves the artwork rather than the detection system is to take advantage of multiplexing. That is, co-collection of multiple point-based imaging spectroscopy modalities is more efficient if the spectral collection time of each modality is long. For example, scanning an area of 1 m^2 at 1 mm^2 spatial sampling, and 100 ms integration time would take approximately 28 h. Each additional point-based modality would require an additional 28 h if collected at the same spatial sampling and integration time. By collecting data from each point-based modality at the same time, the total collection time is significantly reduced.

The decision to co-collect reflectance spectra is based on a long demonstrated synergy between XRF, which provides elemental information, and reflectance spectroscopy, which provides molecular information (i.e. electronic transitions and absorption features associated with vibrational modes) (1, 5–7). In these studies a registration took place between the data collected from the XRF scanner and independently obtained reflectance image cubes collected using high efficiency (640–1000 spatial pixels along the slit) and high spatial sampling hyperspectral cameras (0.16–0.3 mm^2/pixel). While the high spatial information provides useful information, especially related to compositional changes, preparatory sketches and painterly techniques, the spectral information from limited spatial resolution systems are still of great value if the signal to noise ratio in the spectral data that is collected is large enough. Many remote imaging spectrometers operate under these conditions, featuring sub-pixel extraction of spectral signatures of different materials within a single pixel.

For the dual-modal scanner a point-based FORS spectral radiometer was chosen to cover the 350–2500 nm at high spectral sampling (1 and 2 nm). The rationale for collecting spectra over this full range is because electronic transitions in the near UV/visible spectral region can be used to identify numerous inorganic and organic pigments. The spectral features in the 1000–2500 nm near-infrared region provide information on vibrational transitions (combination and overtone features) of various functional groups, such as hydroxyl, carbonate and methyl groups, allowing for more complete identification of pigments and even paint binders [7].

The information provided by FORS spectra (350–2500 nm) nicely complements the elemental information provided by XRF spectroscopy. At least two studies have shown the utility of collecting and making reflectance and elemental maps to identify artists' materials either by fusion of the data through automatic image registration and direct comparison of reflectance and XRF spectra [5], or by fusion of pigment maps generated automatically and separately from the XRF and reflectance spectral features [8]. In the latter case, an improved final pigment assignment was achieved when the independent pigment assignment maps from XRF and reflectance spectroscopic imaging were mathematically combined.

The construction of an integrated scanning system that utilizes both point-based modalities will be discussed here.

Experimental

Physical setup

The National Gallery of Art integrated scanner consists of a high-precision, two-axis, computer-controlled easel, and point collection XRF and FORS instruments. The easel was constructed by SmartDrive, UK (now SatScan Ltd) and has two linear encoders that provide x, y positional information and allow continuous scanning of a 1.7×1.4 m^2 area with step size of 0.01 mm. The XRF instrument consists of a rhodium X-ray source (XOS, East Greenbush, NY, USA) with converging polycapillary optic, and a silicon drift detector with a digital pulse processor (Vortex-90EX, SII DPP, Hitachi High Technologies Science America, Inc.). The FORS instrument consists of an optical fiber spectroradiometer (ASD FS3) and an external tungsten halogen lamp source (Plant Probe), both from Malvern PANalytical, USA.

The configuration of the XRF and FORS sources and detectors are shown in Fig. 1. An attenuated diode laser (Thor labs, NJ) and camera with a 25 EFL mm lens is used to monitor the area being scanned as well as the distance between the artwork and the XRF detector. The top-level system performance detection parameters for both modalities are summarized in Table 1.

In the initial configuration the X-ray source used was the rhodium tube of ARTAX or Bruker AXS Inc instrument operating at 50 kV and 0.5 mA. This source has been replaced with a higher current rhodium X-ray excitation source also operated at 50 kV but with a current of 0.75 mA as noted above. The X-ray beam is aligned normal to the painting surface, and the X-ray detector is oriented at 45° from the normal. The illumination spot sizes can be adjusted from 0.1 to 1 mm in diameter separately from the position of the detector. The front edge of the XRF detector collection tube is adjusted to be 5–10 mm from the painting surface, depending on the height of the impasto. Since the distance from the X-ray source to the painting surface controls the spot size, the entire XRF sensor (source, detector and laser and monitoring camera) is mounted on a translational table with manual micro-motion adjustment to set the separation between the XRF sensor and the painting. Since the system is used only for 'qualitative mapping' the integrated count rate is the key performance metric to compare system efficiency. Using a Röntec bronze standard (Cu 76.8%, Sn 8%, Pb 12%, Zn 1.1%, Sb 0.5%, As 0.02%) an integrated rate of 900 k counts in 1 s was measured for the Rh tube set to a 1 mm diameter spot size, 50 kV and 0.75 mA.

The FORS collection system has an optical fiber bundle that feeds three spectrometers within the FS3 spectral radiometer and is mounted normal to the painting surface. The optical fiber is 1 mm in diameter with a divergent collection angle of 0.43 rad (25°) thus giving a spot size of ~3 mm in diameter at a standoff distance of 4 mm. The illumination system uses a tungsten halogen light source that diffusely illuminates a 2×3 cm^2 elliptical spot at 45° from the painting normal, which can be baffled down to ~1 cm^2. The light level is approximately 5000 lux and the total exposure time is approximately 7 s at any scanned spot on the painting. When internally triggered, or free running, the spectral radiometer acquires spectra at 10 Hz. However, when externally triggered, the collection and saving of spectra is limited to 1 Hz. For the conditions here the spectrometer was triggered at 1 Hz which allowed the averaging of four spectra each having a 134 ms integration time along with the saving of the average spectrum. The light source has a peak spectral radiance of 0.18 W/m^2-sr-nm at 1000 nm. The standard deviation from a 99% diffuse reflectance standard with 134 ms integration time and 4 averages over a small area (~30 pixels) in units of reflectance were 0.57% standard deviation from 350 to 400 nm, 0.05% from 400 to 1700 nm and 0.14% from 1700 to 2300 nm.

The computer controlled easel system consists of a 2-D aluminum easel, controller, and GUI running on a desktop computer. The easel is constructed from 8×4 cm^2 extruded aluminum and is mounted vertically and offset 1 m from the wall. The painting is mounted on a carriage having dimensions of 1.6 by 1.7 m^2 that has three independent clamps that hold the painting from the top. The painting is in contact with small clips on the front of the lower ledge of the carriage to ensure the painting is aligned in a plane that is normal to the XRF source. The carriage can accommodate paintings weighting up to 70 kg. The easel allows for continuous scanning of an area of 1.7×1.4 m^2 (horizontal by vertical). Two optical encoders, one vertical and one horizontal provide positional information at the micron level. Repeat positional precision is ± 50 micrometers or better. The easel is controlled by a GUI which allows the user to specify the dimensions of the area of the art work to be scanned and what scan mode to use; "step and hold" for framing array cameras, "line scan" for push-broom hyperspectral scanners and "raster scan" for single pixel sensors such as the XRF and FORS sensors described here. In raster scan mode the sample size at the painting is needed along with the scan rate; for reasons of efficiency, scanning is done in a boustrophedonical (serpentine) manner. In all scan modes, a text file is produced by the easel software containing all the x, y positions (in the plane of the art work) at which the triggers to the camera or instruments

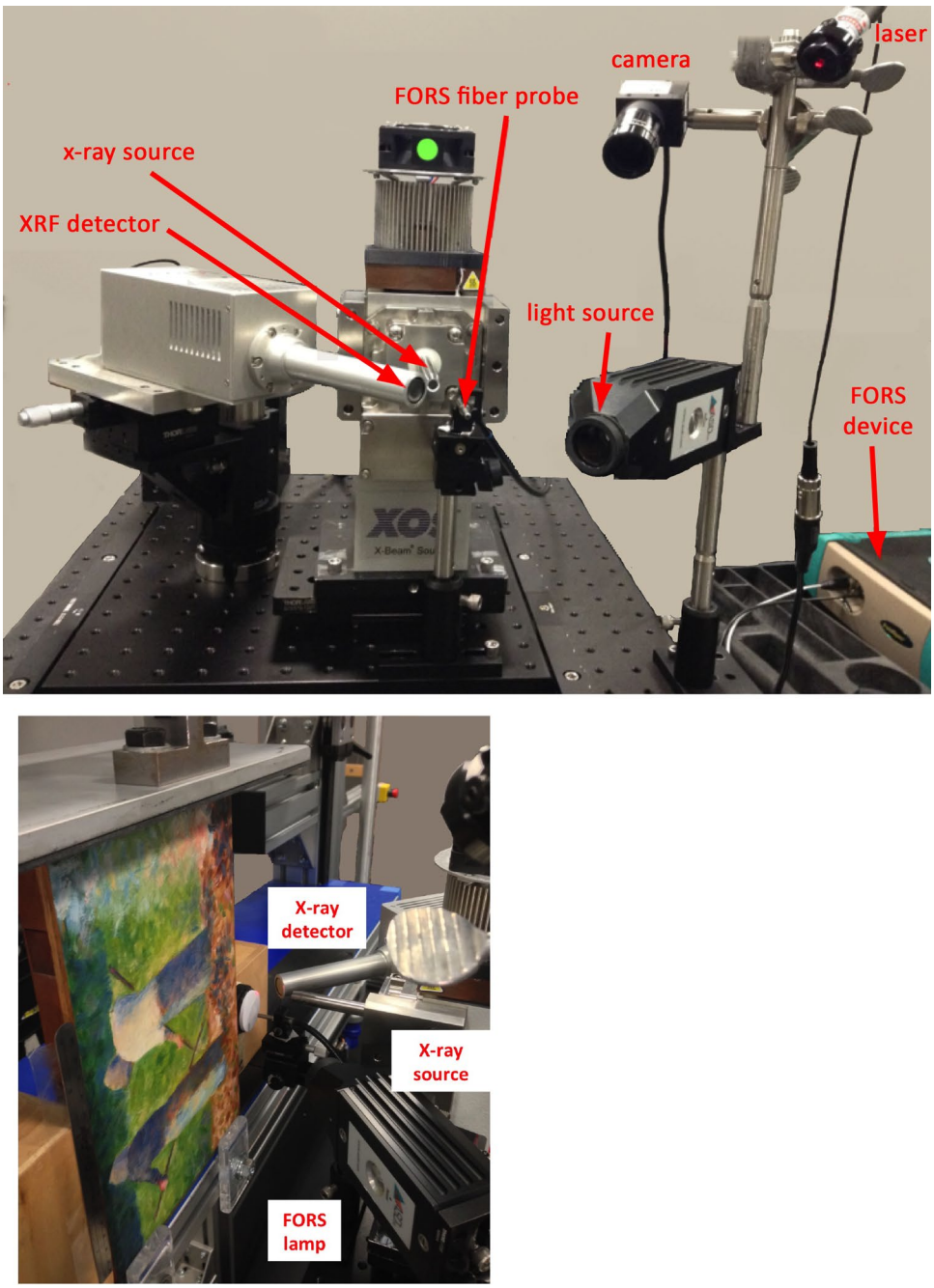

Fig. 1 (Top) a photograph of the view from the painting of the XRF and FORS point measurement collection head showing the X-ray source, X-ray detector and fiber optic reflectance sensor and light source. (Bottom) a photograph showing the painting on the computer controlled easel along with the diffuse white standard and the XRF and FORS instruments

were sent. This positional information allows the spatial re-assembly of the image data. Since the positional information is from two linear encoders physically attached to the easel frame, it is absolute, not relative.

A systems-level block diagram of the XRF and FORS scanner is shown in Fig. 2. The easel controller provides the trigger TTL pulse based on 2-D positions and not on time stamp data, for the collection of the FORS and XRF spectra. The XRF detector used here requires a software trigger; a microcontroller (Arduino ATmega2560) was programmed to send a signal to the desktop computer via a serial (USB) connection. A second microcontroller

Table 1 Detection parameters

Mode	Spectral range	Spectral sampling	Spectral response FWHM	Spatial sampling diameter (mm)	XRF and FORS integration times (s)	XRF only integration times (s)
Reflectance	350–2500 nm	1.4, 350–1050 nm	3 @ 700 nm	3–5	1	NA
		2, 1000–2500 nm	10 @ 1400 nm			
XRF	1.6–25 keV	13.7 eV/channel	165 eV @ Mn K alpha	0.1–1	0.33	0.01–2

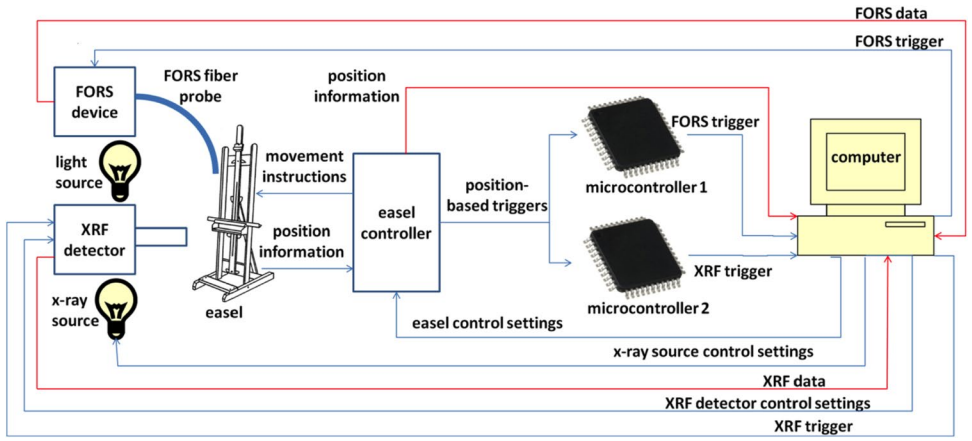

Fig. 2 Block diagram showing the key instruments and interfaces of the XRF and FORS scanner

(Arduino ATmega2560) for FORS triggering is used to divide down the triggers output from the easel given that the FORS spectrometer collection rate is limited to 1 Hz. Typically the XRF scanner is operated at 3 Hz and the FORS spectrometer at 1 Hz.

Two graphical users interfaces (GUI) are used to set up and run the collection of the XRF and reflectance spectral data sets. The easel GUI sets the spatial positions to scan the artwork, along with the desired pixel size at the painting and scan rate (i.e. pixel size at the artwork divided by the XRF integration time). This can be varied from ~1 mm/s to 50 mm/s (safety limit). A separate custom GUI for monitoring the XRF spectra collection displays the sum spectrum at the end of each scan line and a map of the emerging image from the intensity at one emission energy value. The vendor supplied FORS GUI is used to see each average spectrum saved.

Formation of XRF and reflectance image cubes

The raw XRF and FORS image cubes are created directly from the acquired spectra and from the positional information obtained from the scanner. As in all scanning systems where the scanner does not stop for each spectral acquisition operation, the actual position at which the data is acquired varies with scan speed. Thus, the samples may not be collected on a regular fixed grid. A bi-cubic interpolation function is used to resample the raw data to a regularized (x, y) grid. Since the ideal interpolator for such a case would be a sinc function, the use of a bi-cubic function introduces little error.

The final XRF and reflectance image cubes can be exploited directly. However, the determination of elemental maps from the XRF data cube, more specifically emission maps, obtained from integrating the counts from each detected emission peak has been found to be most useful [12–14]. To ensure the broad background and the response function of XRF detectors, which allow for contributions from more than one emission peak to be collected in a specific energy bin, do not lead to errors in the maps due to elemental overlaps, various fitting strategies and software have been developed [12–14] and are commonly used.

As the National Gallery of Art's XRF scanner was initially developed in 2014, more empirical fitting software was programmed at the time in which each XRF spectrum is fit to a sum-of-Gaussian-peak group functions [8].[1] While such an approach is not new, it has certain

[1] The XRF spectral fitting and map-making software tool as well as the control GUI for collecting the XRF cubes is available as open source software and can be obtained by emailing the corresponding author.

advantages of being fast and requiring little user interaction. The user needs to identify the elements expected, obtained by examining the raw cube and using a priori knowledge of the pigments available in the time period the artwork originates from. Since the energy of each element's emission lines is known (E_g), and the XRF detector response function width as a function of peak energy is also known (ω_g, the peak full width at half maximum (FWHM)), the position and width of the Gaussians are considered to be known a priori. Only the amplitudes (A_g) and offsets (C_g), which represent the local baseline below the peak/s, are unknown and best-fit values for these parameters need to be determined. To ensure a robust fit, however, the width of the response function (ω) is also fitted, with the simplification that ω is locally constant over narrow energy ranges (we fit a single value, rather than one value per element, in regions of overlap). Thus these values are determined by nonlinear regression of the function,

$$f\left(E, A_{1..G}, \omega, C; E_g\right) = \sum_{g=1}^{G} A_g e^{\frac{-4\ln(2)\left(E-E_g\right)^2}{\omega^2}} + C_g \tag{1}$$

to the spectral data, where G is the number of emission peaks in the spectral region being fit.

XRF elemental image maps for each emission line represent the area under the fitted Gaussians to the emission peaks. The presence of pigments are typically inferred based upon the elemental composition, and also using the visual color to guide the assignment.

Since the FORS instrument was calibrated to apparent reflectance using a diffuse 99% white reflectance standard prior to the data collection, no further calibration was required before making material maps. Maps of pixels with similar reflectance spectra are made using algorithms such as the spectral angle mapper (ENVI) as done here. In brief, the reflectance spectrum at each pixel can be represented as a point in n-dimensional space where n is the number of spectral bands in the spectral region being analyzed. A vector can be drawn from the spectrum point through the origin. The spectral angle mapper (SAM, ENVI Software) routine returns the angle between the spectra of each pixel in the image cube and the reference spectrum. A small angle means a close match and a high intensity value in the SAM false color images. The limiting angle for the SAM images was determined by examining the histogram of angles returned by the SAM routine. A typical threshold angle was set to be on the rising edge of the histogram or the first peak of a multi-peaked histogram. The spectra of the pixels obtained from these settings were examined to ensure the selected angle, used by the SAM routine, identified only spectra having the characteristic feature/s of the pigment of interest. Typical threshold angle values (i.e. the values below which a "close match" is assigned) ranged from 0.02 to 0.12 radians. Such maps can be compared with the XRF elemental maps in order to assign pigments to them. Note, the limiting angle is found to vary for each reflectance spectrum mapped.

The reflectance maps presented here were calculated using SAM with a portion of the spectral range that contained the key spectral feature/s characteristic of the material to be mapped. The list of pigments and spectral ranges are as follows: lead white 1435–1455 nm, vermilion 550–630 nm, red ocher 410–904 nm, cobalt blue 640–1865 nm, and viridian 450–1000 nm.

Results and discussion

Two examples of hyperspectral image cubes collected with the dual-mode scanner are presented. The first involves the collection of only XRF spectral image cubes from a large warped panel painting and the second a small panel painting where both XRF and reflectance spectral image cubes were recorded.

Elemental maps were obtained from Andrea del Sarto's *Charity*, (before 1530), in the collection of the National Gallery of Art, Washington, DC (Fig. 3). The painting is 1.2×0.93 m^2 in size and is on an un-cradled thick wooden panel, which is warped and is roughly barreled shape, curving away towards the edges and corners. The panel was mounted vertically on the easel, and held in place by three vertical clamps at the top of the painting. The painting is in contact with three small clips on the lowest ledge of the easel carriage. This allowed the painting to remain in the same place for the collection period required. Over the area of interest, 0.7×0.72 m^2, the high point of the painting occurs in the center and the panel curves away by -6 mm at the bottom left corner and -5 mm on the bottom right corner (z-axis direction, normal to the painting).

A sensitivity test using the copper peak (Cu-Kα) intensity from a spot on the painting was used to determine the change in signal with displacement of the XRF sensor in the z-axis. At the optimal z-position a count peak rate of 28 k counts per second (cps) was measured. A set of measurements when z was varied yielded a slope of 1589 cps per mm displacement in z. The count rate increased when moving towards the painting and decreased when moving away from it. Setting an acceptable variation of $\pm 10\%$ meant that the areas scanned should remain ± 2 mm from the nominal position in z. Six rectangles of different dimensions on the painting were determined and scanned over several days with the nominal z position adjusted for each. The data collection was done with a 1 mm diameter spot size and 100 ms integration time,

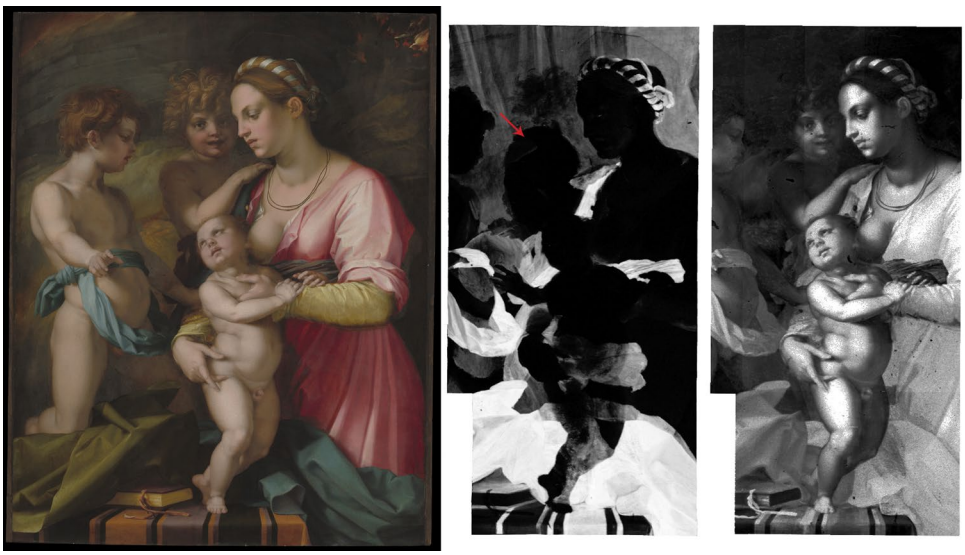

Fig. 3 (Left) color image of Andrea del Sarto's *Charity,* Samuel H. Kress collection, National Gallery of Art, Washington D.C. Photo Mr. G. Williams, (middle) Copper (Cu Kα) map, (right) inverted natural log of Iron Kα map. Dark areas denote where iron was found. Note in the Cu Kα map the head of a man can be seen in reserve (red arrow), in the area of the chest and chin of the boy in the middle of the painting

or a scan speed of 10 mm/s. Because the easel provides a text file of absolute positions in x, y of all the spectra collected, the six data collections could be directly combined to make the full image cube [15].

Elemental maps (Fig. 3) calculated from the image cube using Eq. 1 show a good signal to noise ratio was obtained by the scanning system, giving rise to uniform integrated maps. Of particular interest in the XRF elemental maps is the reserve left for the head of a man in the copper map (Fig. 3) not apparent in the finished painting. The reserve appears to be behind the chest and chin of the central child. The painting was XRF scanned along with the collection of an infrared reflectogram (150 dpi) for comparison with a del Sarto painting titled *Borgherini Holy Family,* in the collection of Metropolitan Museum of Art. In that painting, St John the Baptist is present as a man whereas in *Charity* he is a young boy. Comparison of the XRF maps and infrared reflectograms of both paintings show that these works are closely related as is discussed by Bayer et al. [16].

As a second example, a portion of the painting *Haymakers at Montfermeil* (total painted area 24.8 × 15.6 cm, c. 1882) by Georges Seurat was scanned (17.7 cm width × 16.8 cm height) and both XRF and reflectance spectra were collected. The dimensions of the area to be scanned, the spot size (1 mm dia. for XRF) and the scan rate (3 mm/s) were entered into the easel GUI controller along with the positional starting point. The total scan time was 3 h. Using the positional information from the computer-controlled easel, both the reflectance image cube and XRF image cube were constructed. A false-color image obtained from the reflectance image cube is given in Fig. 4, along with reflectance and XRF spectra from the same site, i.e. the shoulder of the woman in the blue shirt. These two point-based spectra demonstrate the complementary nature of reflectance and XRF spectroscopies. The XRF spectrum is dominated by elemental emission from lead and cobalt, with less intense XRF emission from iron and chromium. The associated reflectance spectrum confirms the blue color is dominated by cobalt blue [17]. Specifically, the broad absorption in the near infrared from approximately 1160–1600 nm as well as small absorption features in the visible (approximately 545, 585, and 625 nm) is characteristic of cobalt blue. These features originate from the ligand-field transitions between the d–d orbitals of Co(II) in a pseudo-tetrahedral configuration. Cobalt blue does not absorb much light between 700 and 1000 nm and thus displays a sharp increase in reflectance at around 690 nm with a local reflectance maximum near 850 nm. In the reflectance spectrum shown, however, a broad absorption from 660 to 1120 nm indicates that another pigment is present. Iron ochre and/or umber absorb in this spectral region, and are likely affiliated with the small iron peak seen in the XRF spectrum. The strong near-infrared absorption of cobalt blue in the reflectance spectrum nearly masks the weak absorption at 1445 nm, typical of the hydroxyl group of basic lead white [8], unlike the XRF spectrum, in which the lead peaks were the most intense. Analyzing the information from both modalities provides a more

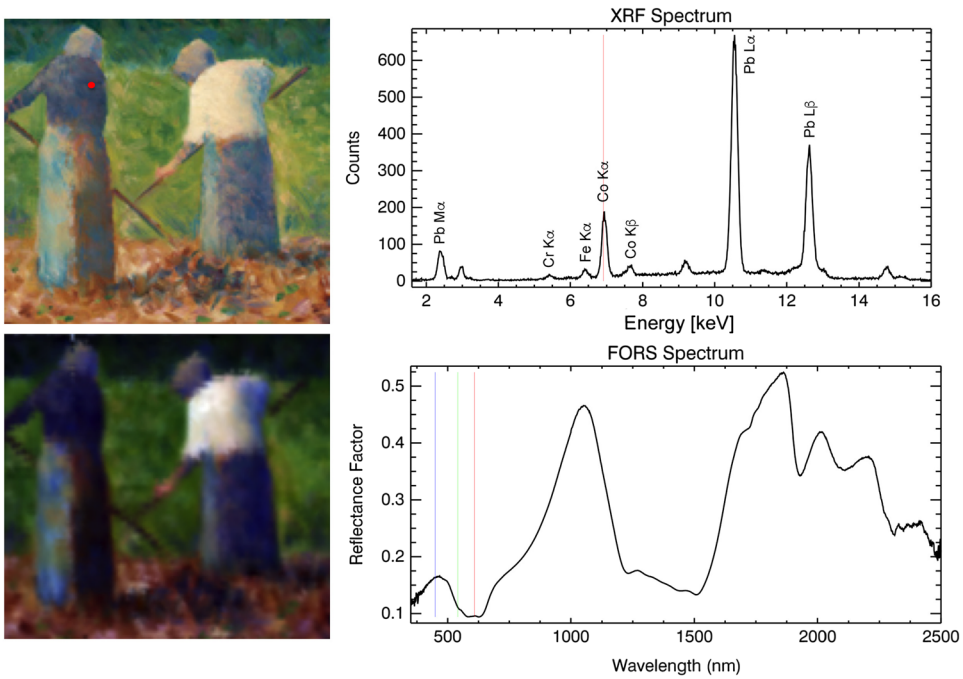

Fig. 4 (Top left) detail color image of Georges Seurat's *Haymakers at Montfermeil* (1882). Collection of Mr. and Mrs. Paul Mellon, 2014.18.48, National Gallery of Art, Washington, D.C. Photo Mr. G. Williams, (Bottom left) false-color image (450, 550, 620 nm) created from the FORS cube, (Top right) single spectrum from the scanned XRF data (at the point marked with a red dot), (Bottom right) single spectrum from the scanned FORS data (at the point marked with a red dot)

complete picture of the pigments used (in this example, cobalt blue, lead white and an iron oxide pigment).

Analysis of both the XRF and reflectance image cubes revealed evidence supporting that lead white was used throughout the entire painting. The XRF Pb-L_α map (Fig. 5b) shows the presence of lead across the painting. The lead observed here is likely to be associated with commercial lead white (mostly basic lead(II)-carbonate) or possibly red lead. The reflectance spectrum of basic lead(II)-carbonate has a characteristic narrow absorption feature at 1446 nm from a vibrational overtone associated with the hydroxyl group [18] (Fig. 5c). A map of this hydroxyl feature (Fig. 5d) shows the presence of lead white in many of the same areas as the XRF map. For example, the white blouse of the woman to the right and the lighter blue passage of the skirt of the woman to the left are painted using lead white. The areas in the painting having little or no lead white correspond to areas in the reflectance map of which the reflectance spectra show little or no absorption at 1446 nm (Fig. 5d). The lack of absorption at 1446 nm in the reflectance spectra is either due to a lack of basic lead white or the presence of a more strongly absorbing pigment in this spectral region. This is an advantage of having both modalities, as the XRF map shows lead, presumably from lead white, across many of the spatial areas that appear dark in the reflectance map. As shown below, many of the 'dark' areas in the reflectance map correspond to the blue-colored areas of the artwork. These blue areas are painted with cobalt blue, which has a strong absorption in the same near-infrared spectral region as basic lead white. Thus, the presence of cobalt blue may hinder the detection of lead white if using only reflectance spectroscopy. The reflectance spectra and maps are still useful though, because when the 1446 nm absorption feature is detected, it confirms that the XRF-detected lead is present as lead white. In addition, the reflectance spectra and maps provide a better indication of the pigments mainly responsible for the observed color of the painting, which is more difficult to discern if only looking at the XRF elemental maps. Note that zinc white was ruled out as a possible white pigment, as neither x-ray fluorescence of zinc nor a reflectance transition edge near 380 nm (indicative of zinc white's band gap absorption) was detected. This is an advantage of extending the reflectance scanner to 350 nm as zinc white and both forms of titanium dioxide can be detected on the surface of the painting [7].

The iron (Fe) elemental map (Fig. 6b) shows the presence of iron in the leaves on the ground and on the shadowed skirt of the woman in the blue shirt. Since iron is used in ochres and umbers, further specificity can be obtained by looking for characteristic absorption

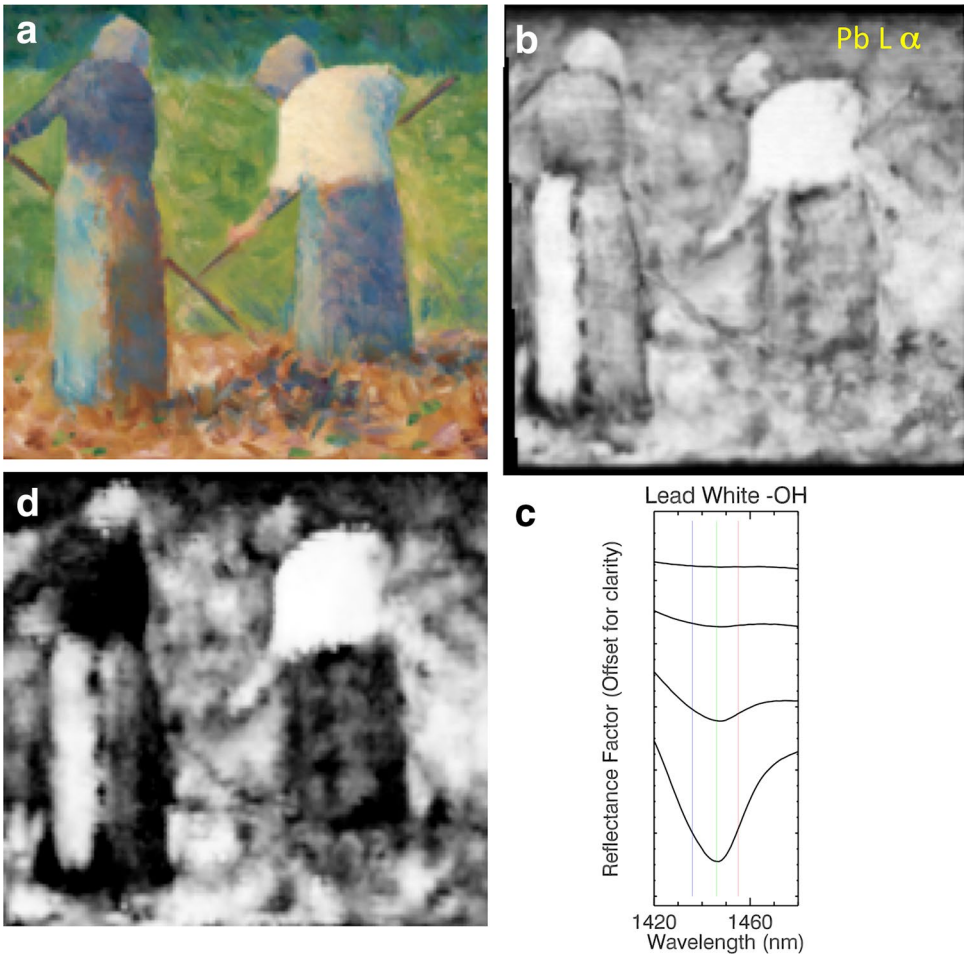

Fig. 5 **a** Detail color image, (**b**) The XRF elemental map of lead (Pb) L-alpha emission, (**d**) reflectance map of hydroxyl feature of lead white at 1446 nm, where "white" and "gray" areas indicate the presence of the 1446-nm lead white absorption and "black" areas indicate the lack of this spectral feature. Map obtained using SAM algorithm and equalization of histogram applied. **c** Reflectance spectra from "white" (bottom of plot) to "black" (top of plot) areas in reflectance map

features in the reflectance spectra. The reflectance spectrum (Fig. 6d, green spectrum) has a reflectance transition edge at around 560 nm and broad absorptions near 640 and 850 nm that result in a local reflectance peak at 760 nm, which is characteristic of the iron oxide hematite [1, 6, 19]. Using this reflectance spectrum to query the cube for spectral matches from 400 to 900 nm with the spectral angle mapper algorithm shows that the reddish brown leaves in the foreground were painted with hematite (Fig. 6e, green).

Interestingly, the elemental map (Fig. 6c) for mercury (Hg), likely from vermilion (HgS), shows little mercury is associated with the reddish leaves, and in the few areas of the leaves where some is detected, the associated reflectance spectrum is dominated by the spectral features of hematite. The hand of the woman in the white shirt does contain mercury and the associated reflectance spectrum shows a sharp transition edge at 585 nm indicative of vermilion (Fig. 6d, red spectrum). It should be noted that the transition edge of vermilion has been found to vary from 580 to 600 nm, but it is sharp (with a first derivative FWHM of less than 40 nm) [6]. The red areas in the reflectance map (Fig. 6e) are a match to the reflectance spectrum of vermilion and occur for the same hand that was identified in the XRF data as containing mercury. Some of the slight discrepancies between the XRF elemental maps and the reflectance maps may occur because the XRF maps can show the distribution of pigments below the surface (depending on matrix effects), whereas the reflectance maps show pigments that are closer to the surface because reflectance spectral features in the visible were used for mapping.

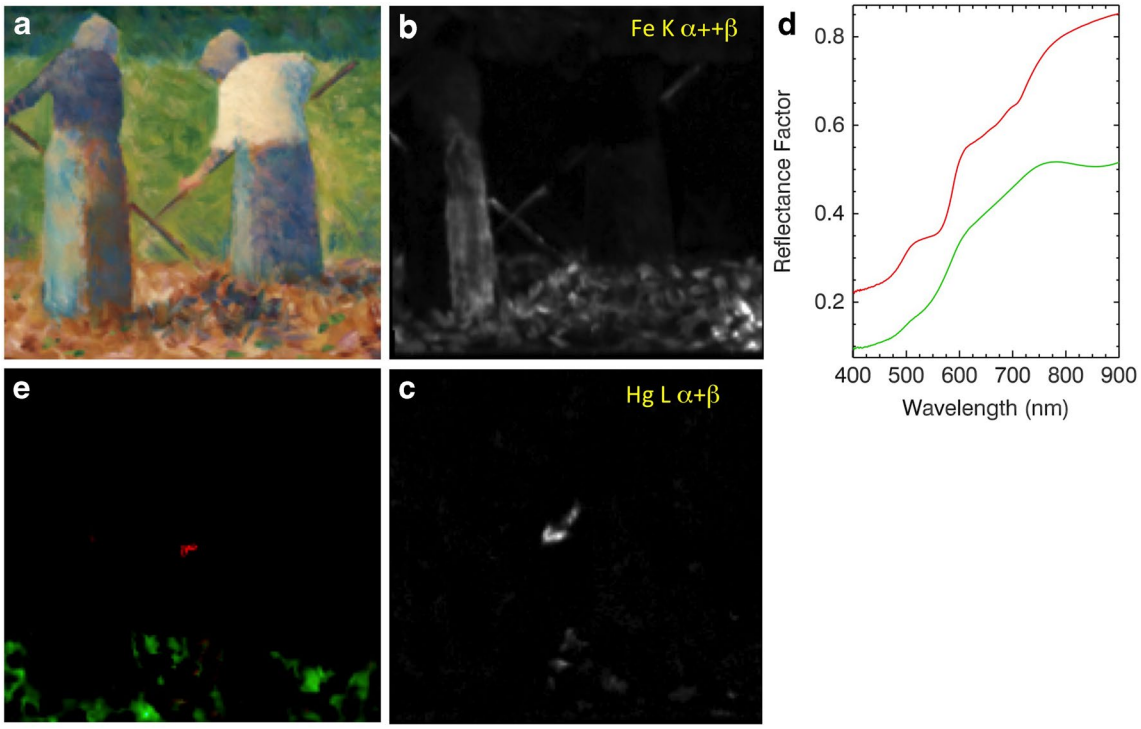

Fig. 6 **a** Detail color image, XRF elemental maps of (**b**) iron, Fe, and (**c**) mercury, Hg, (**d**) reflectance spectra containing hematite (green), vermilion (red) and associated (**e**) false-color map obtained using the SAM algorithm with the intensity values linearly stretched

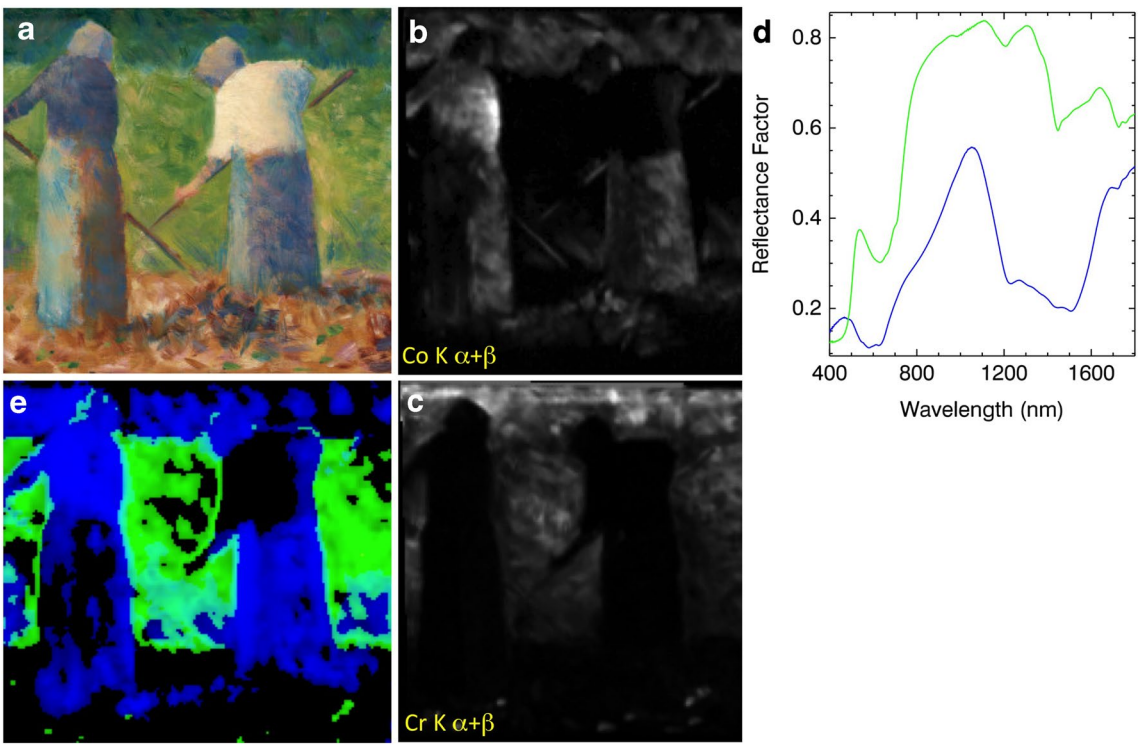

Fig. 7 **a** Detail color image, XRF elemental maps of (**b**) cobalt, Co, and (**c**) chromium, Cr, (**d**) reflectance spectra of cobalt blue (blue) and viridian (green) and associated (**e**) false-color image map obtained using the SAM algorithm with the histogram equalized

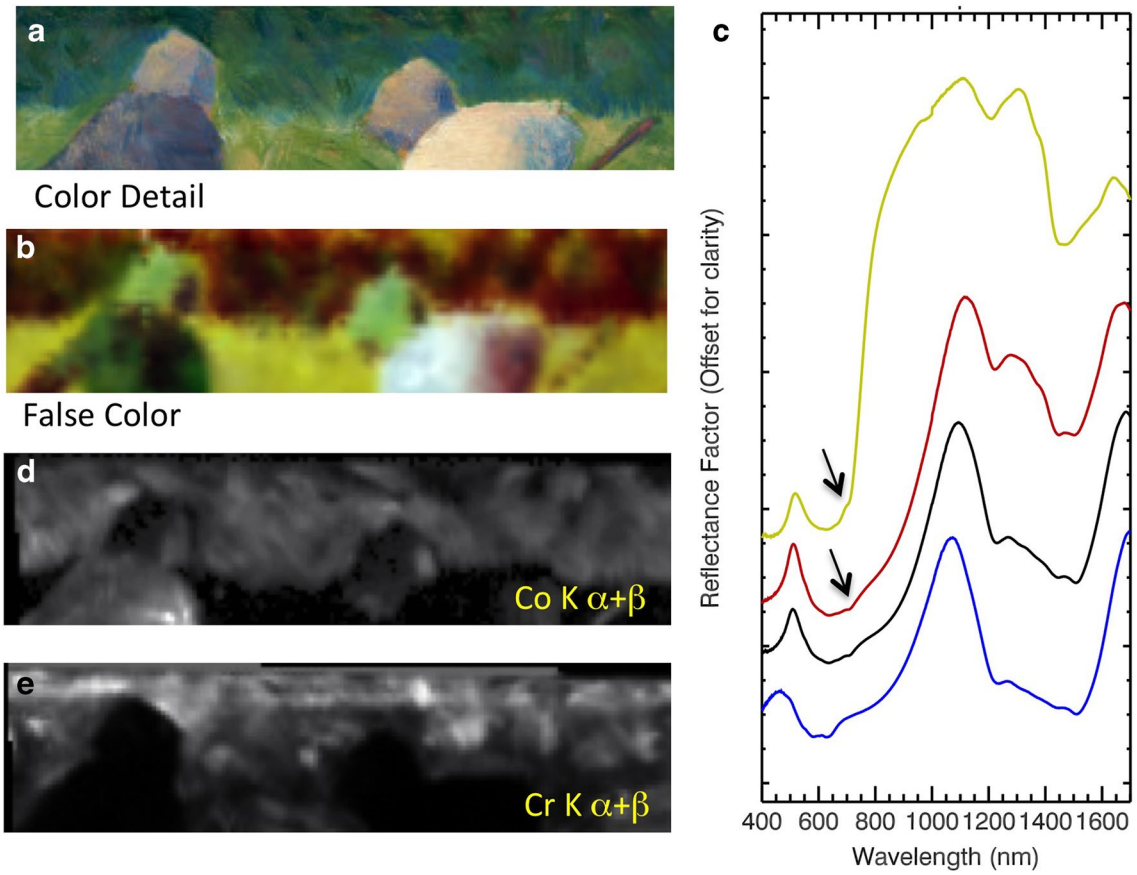

Fig. 8 **a** Detail color image of the trees at the top of the painting. **b** False-color image (RGB, 1250, 850, 650 nm), **c** reflectance spectra of viridian (yellow), cobalt blue (blue), and the combination of viridian and cobalt blue: less cobalt blue to viridian (red), more cobalt blue than viridian (black). Relatively pure viridian was used for the grass, but a mixture of viridian and cobalt blue was used for the trees. The arrow points to the absorption shoulder characteristic of viridian. XRF elemental maps of **d** cobalt, Co, and **e** chromium, Cr.

The cobalt (Co) elemental map (Fig. 7b) reveals a wide use of a cobalt-based pigment or pigments in the composition; for example, in the blouse of one woman and the skirt of another, as well as areas in the leaves, grass, and trees at the top edge of the painting. Possible cobalt-based pigments that could have been used include cobalt blue, cerulean blue, and even smalt, although this would have been unlikely in the nineteenth century. Since no tin (Sn) was found in the elemental maps, cerulean blue is not present, but smalt or cobalt blue are possible. Each of these pigments has a distinct reflectance spectrum associated with electronic transitions in the near infrared [17]. The characteristic reflectance spectra from the deep blue-colored areas of the painting (Fig. 7d) have a broad, near-infrared absorption from ~1227 to 1506 nm that indicate a match to cobalt blue. The spectra also show weak visible absorption bands associated with ligand-field transitions of cobalt blue as well (546, 582, 623 nm). The reflectance map for cobalt blue (Fig. 7e) shows a good match to the cobalt elemental map indicating the Co-containing pigment used in these regions is cobalt blue.

The chromium (Cr) elemental map (Fig. 7c) matches up with the green field, a few green leaves among the red-brown leaves, and into the tree line where cobalt was also detected. The possible green pigments include chromium oxide and viridian (hydrated chromium (III) oxide). The reflectance spectra from the green field have an absorption feature at 705 nm and a sharp inflection point at 750 nm, which matches well with viridian green and not with chromium oxide [20]. The reflectance map for viridian green shows its presence in the grass but not in the greenish portion of the trees at the top of the painting where Cr was detected in the XRF map. This material discrepancy in the trees was further examined in Fig. 8. Examination of a false-color image (Fig. 8b) constructed from the reflectance image cube reveals that the blue-green trees at the top of the painting are mainly painted with a mixture of cobalt blue and viridian (red and black spectra in Fig. 8c).

Conclusions

This paper presents the design and construction of an imaging spectroscopic scanner capable of collecting XRF and FORS image cubes. Because the illumination sources and detectors remain immobile while instead the painting is moved, multiple point-based spectroscopy modalities can easily be added or tested. While higher spatial resolution and shorter collection times can be obtained with hyperspectral reflectance imaging cameras or high flux X-ray sources, this paper shows the utility of a moderate spatial resolution imaging system to map the chemical composition of painted works of art in a museum environment. Moreover, this approach eliminates the need to purchase two hyperspectral reflectance cameras that operate together to cover the spectral range from 400 to 2500 nm since the FORS instrument used here is sensitive over this entire spectral range. Although hyperspectral reflectance cameras can provide < 0.2 mm spatial sampling with 500× to 1000× faster collection speeds, the relatively higher cost of the imaging cameras may be prohibitive for many institutions. Thus using the FORS instrument as the reflectance modality makes for a relatively lower cost, dual imaging modality XRF and FORS scanner.

Authors' contributions

DMC, JKD and ML designed and implemented the FORS scanner. DMC, LDG, JKD and KJ designed and built the XRF scanner. DMC developed and wrote the GUIs. JKD, KAD, DMC conducted the experiments, and JKD, DMC, KAD, LDG did the data analysis. JKD and DMC, with help from the coauthors, wrote the paper. All authors read and approved the final manuscript.

Author details

[1] Department of Scientific Research, National Gallery of Art, Washington, DC 20565, USA. [2] School of Engineering and Applied Science, George Washington University, Washington, DC 20052, USA. [3] Present Address: Sensors and Electron Devices Directorate, U.S. Army Research Laboratory, Adelphi, MD 20783, USA. [4] Department of Chemistry, University of Antwerp, Antwerp, Belgium.

Acknowledgements

The authors acknowledge funding from the National Science Foundation (Award 1041827). J.K.D. and D.M.C. acknowledge funding from the Andrew W. Mellon and Samuel H. Kress Foundations. The authors are grateful to David Martin and Dennis Murphy of SmartDrive Ltd., Gary Fager of Malvern PANalytical, and Gao Ning of XOS for advice. KJ acknowledges support from EU-InterReg project SmartLight and from GOA Project SolarPaint (University of Antwerp Research Council).

Competing interests

The authors declare that they have no competing interests.

Ethics approval and consent to participate

Not applicable.

Publisher's Note

Received: 23 January 2018 Accepted: 9 May 2018
Published online: 30 May 2018

References

1. Delaney JK, Ricciardi P, Glinsman LD, Facini M, Thoury M, Palmer M, de la Rie ER. Use of imaging spectroscopy, fiber optic reflectance spectroscopy, and X-ray fluorescence to map and identify pigments in illuminated manuscripts. Stud Cons. 2014;59:91–101.
2. Alfeld M, Janssens K, Dik J, de Nolf W, van der Snickt G. Optimization of mobile scanning macro-XRF systems or the in situ investigation of historical paintings. J Anal At Spectrom. 2011;26:899–908.
3. Van der Snickt G, Legrand S, Caen J, Vanmeert F, Alfeld M, Janssens K. Chemical imaging of stained-glass windows by means of macro X-ray fluorescence (MA-XRF) scanning. Microchem J. 2016;124:615–22.
4. Alfeld M, Pedroso JV, van Eikema Hommes M, van. der Snickt G, Tauber G, Blass Haschke JM, Erler K, Dik J, Janssens K. A mobile instrument for in situ scanning macro-XRF investigation of historical paintings. J Anal At Spectrom. 2013;28:760–7.
5. Dooley KA, Conover DM, Glinsman LD, Delaney JD. Complementary standoff chemical imaging to map and identify artist materials in an early Italian renaissance panel painting. Angew Chem Int Ed. 2014;53:13775–9.
6. Delaney JK, Zeibel JG, Thoury M, Littleton R, Palmer M, Morales KM, de la Rie ER, Hoenigswald A. Visible and infrared imaging spectroscopy of Picasso's Harlequin musician: mapping and identification of artist materials in situ. Appl Spectrosc. 2010;64:584–94.
7. Dooley KA, Coddington J, Krueger J, Conover DM, Loew M, Delaney JK. Standoff chemical imaging finds evidence for Jackson Pollock's selective use of alkyd and oil binding media in a famous 'drip' painting. Anal Methods. 2017;9:28–37.
8. Conover DM. Fusion of reflectance and X-ray fluorescence imaging spectroscopy data for the improved identification of artists' materials. Ph.D. thesis. The George Washington University (Summer 2015).
9. Jackall Y, Delaney JK, Swicklik M. 'Portrait of a Woman with a Book': a 'Newly Discovered Fantasy Figure' by Fragonard at the National Gallery of Art, Washington. Burlingt Mag. 2015;157(1345):248–54.
10. Ravaud E, Pichon L, Laval E, Gonzalez V, Eveno M, Calligaro T. Development of a versatile XRF scanner for the elemental imaging of paintworks. Appl Phys A. 2016;122:17.
11. Romano FP, Caliri C, Nicotra P, Di Martino S, Pappalardo L, Rizzo F, Santos HC. Real-time elemental imaging of large dimension paintings with a novel mobile macro X-ray fluorescence (MA-XRF) scanning technique. J Anal At Spectrom. 2017;2:773–81.
12. Alfeld M, Janssens K. Strategies for processing mega-pixel X-ray fluorescence hyperspectral data: a case study on a version of Caravaggio's painting Supper at Emmaus. J Anal At Spectrom. 2015;30:777–89.
13. Vekemans B, Janssens K, Vincze L, Adams F, Van Espen P. Analysis of X-ray spectra by iterative least squares (AXIL)—new developments. X-Ray Spectrom. 1994;23:278–85.
14. Solé VA, Papillon E, Cotte M, Walter P, Susini J. A multiplatform code for the analysis of energy-dispersive X-ray fluorescence spectra. Spectrochim Acta Part B. 2007;62:63–8.
15. Conover DM, Delaney JK, Loew MH. Automatic registration and mosaicking of technical images of Old Master paintings. Appl Phys A. 2015;119:1567–75.
16. Bayer A, Gallagher M, Centeno SA, Delaney JK, Read E. Andrea del Sarto's Borgherini holy family and charity: two intertwined late works. Metrop Mus J. 2017;52(1):34–55.
17. Bacci M, Magrini D, Picollo M, Vervat M. A study of the blue colors used by Telemaco Signorini (1835–1901). J Cult Heritage. 2009;10:275–80.
18. Bacci M, Picollo M, Trumpy G, Tsukada M, Kunzelman D. Non-invasive identification of white pigments on 20th-century oil paintings by using fiber optic reflectance spectroscopy. JAIC. 2007;46:27–37.
19. Clark RN. Spectroscopy of rocks and minerals, and principles of spectroscopy. In: Rencz AN, editor. Manual of remote sensing, remote sensing for the earth sciences, vol. 3. New York: Wiley; 1999. p. 3–58.
20. National Gallery of Art. In-house reflectance spectral database. Washington, D.C.: National Gallery of Art.